nature medicine

TECHNICAL REPORTS

Monitoring photodynamic therapy of solid tumors online by BOLD-contrast MRI

Shimon Gross[1,2,3], Assaf Gilead[1,3], Avigdor Scherz[2], Michal Neeman[1] & Yoram Salomon[1]

Antivascular photodynamic therapy (PDT) of tumors with palladium-bacteriopheophorbide (TOOKAD) relies on *in situ* photosensitization of the circulating drug by local generation of cytotoxic reactive oxygen species, which leads to rapid vascular occlusion, stasis, necrosis and tumor eradication. Intravascular production of reactive oxygen species is associated with photoconsumption of O_2 and consequent evolution of paramagnetic deoxyhemoglobin. In this study we evaluate the use of blood oxygenation level–dependent (BOLD) contrast magnetic resonance imaging (MRI) for real-time monitoring of PDT efficacy. Using a solid tumor model, we show that TOOKAD-PDT generates appreciable attenuation (25–40%) of the magnetic resonance signal, solely at the illuminated tumor site. This phenomenon is independent of, though augmented by, ensuing changes in blood flow. These results were validated by immunohistochemistry and intravital microscopy. The concept of photosensitized BOLD-contrast MRI may have intraoperative applications in interactive guidance and monitoring of antivascular cancer therapy, PDT treatment of macular degeneration, interventional cardiology and possibly other biomedical disciplines.

PDT relies on photoexcitation of an inactive photosensitizing drug in the tissue of interest at a wavelength matched to photosensitizer absorption. The excited photosensitizer reacts *in situ* with molecular oxygen to produce cytotoxic reactive oxygen species, resulting in necrosis of the treated tissue. Photogeneration of reactive oxygen species during the course of PDT is manifested by local photoconsumption of oxygen[1,2] and hemodynamic insults that include capillary occlusion, hemorrhage and stasis[3,4]. These vascular effects are crucial for development of necrosis and tumor eradication[3,4]. PDT represents a relatively new approach to the treatment of various tumors[5] and nonmalignant, hyperproliferative diseases[6] such as ophthalmic age-related macular degeneration, for which PDT is already in wide clinical use[6].

We recently synthesized a new family of photosensitizing agents derived from the photosynthetic pigment bacteriochlorophyll a[1,3,7–12]. The lead compound, TOOKAD, was developed by us in collaboration with Steba Biotech (Toussus Le-Noble, France) and has photochemical and pharmacological characteristics that are superior to those of photosensitizing agents in clinical use. These characteristics include a high molar extinction coefficient (ε_0) at near-infrared (ε_0 of ~10^5 at 763 nm, enabling active treatment depth up to 2 cm)[7,8,10,11] and rapid clearance from the circulation (half-life of 3 min; unpublished data). Vascular targeting is achieved by simultaneous intravenous administration of TOOKAD and illumination of the treatment site, enabling a shorter treatment protocol and intraoperative application[7,8,10,12]. In July 2002, Steba Biotech started clinical trials of TOOKAD-PDT for the treatment of prostate cancer.

We previously reported that antivascular PDT with bacteriochlorophyll derivatives induces appreciable response and cure rates for melanoma, glioma, sarcoma and human prostate xenograft models in mice[3,8,11], rats[9] and normal dog prostate[10].

Precise light delivery is essential for safe PDT. Although optic-fiber insertion into internal organs can be assisted by standard techniques (optical, X ray or ultrasonography), real-time imaging of the light impact and tissue response to PDT is presently unavailable. This may be crucial in cases where the target tumor is internal or located near vital organs, nerve bundles or major blood vessels that must be spared (for example, in multifiber light delivery for treatment of prostate cancer). In such cases, online guidance of the photodynamic process is desirable.

BOLD-contrast MRI was first shown *in vivo* and in deoxygenated human blood *ex vivo* by Ogawa *et al.*[13]. BOLD-contrast MRI of susceptibility-weighted (T_2^*) or transverse relaxation–weighted (T_2) images is derived from the inherent paramagnetic properties of deoxyhemoglobin. Detection and imaging *in vivo* rely on spatial and temporal changes in blood oxygenation, flow and volume[14]. BOLD-contrast MRI has been applied in cancer research for monitoring tumor response to vasomodulators[15], analysis of tumor vessel functionality and maturation, and angiogenesis[15–18].

We therefore examined whether photoconsumption of oxygen and the consequent hemodynamic effects inherent to antivascular PDT could generate detectable BOLD contrast, thus enabling functional MRI of a photochemical process. We tested this concept by evaluating changes in magnetic resonance contrast during TOOKAD-PDT, using the solid M2R mouse melanoma model. We

Departments of [1]Biological Regulation and [2]Plant Sciences, The Weizmann Institute of Science, Rehovot 76100, Israel. [3]These authors contributed equally to this work. Correspondence should be addressed to Y.S. (yoram.salomon@weizmann.ac.il).

Published online 21 September 2003; doi:10.1038/nm940

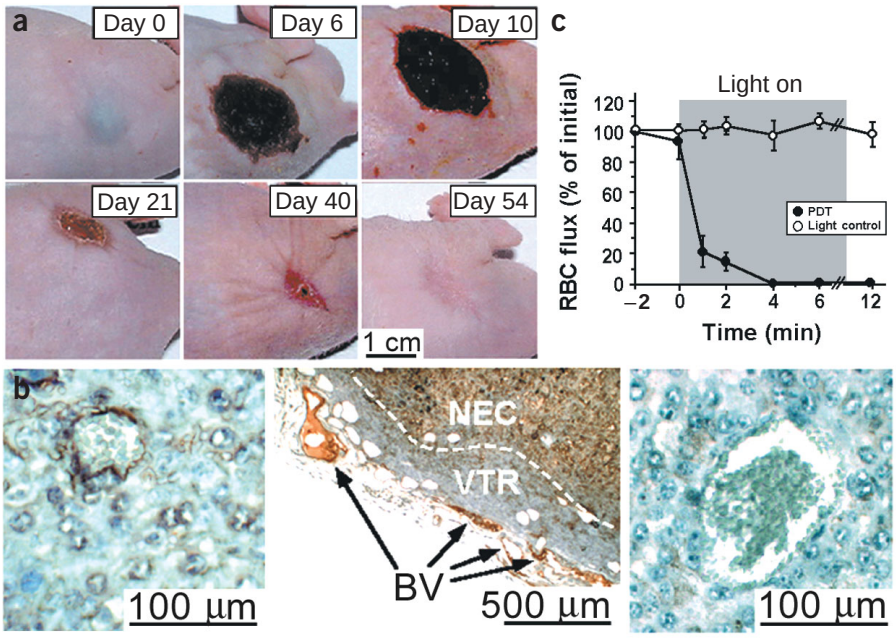

Figure 1 TOOKAD-PDT of M2R mouse melanoma. (**a**) Tumor response in a mouse treated with TOOKAD and immediately illuminated. Complete healing and cure were defined as tumor-free states at 50–60 d and 90 d, respectively, after PDT. (**b**) Immunostaining for PDT-induced vascular lipid peroxidation. Left and middle, positive staining of HNE-protein adducts (brown; indicative of lipid peroxidation). PDT-induced HNE staining is confined to blood vessel wall (left), mainly coinciding with the large vessels (BV) at the viable tumor rim (VTR; middle). HNE staining is also observed in the spontaneous necrotic core (NEC) of the tumor (PDT-independent; middle). Right, negative staining in light-control animals. Histological sections were prepared from three PDT-treated, two light-control and two dark-control (data not shown) mice. Representative specimens are shown. (**c**) Tumor perfusion, as determined by red blood cell (RBC) flux in PDT-treated ($n = 6$) and light-control ($n = 5$) mice, was monitored by video microscopy in animals administered red blood cells prestained with ~1% 4-Di-10-ASP and dextran-TRITC as a blood-pool marker.

show here the generation of considerable BOLD contrast at the tumor site upon TOOKAD-PDT.

RESULTS

TOOKAD-PDT of solid M2R melanoma

Solid subcutaneous tumors derived from the M2R melanoma cell line were treated with TOOKAD-PDT. A single PDT treatment induced hemorrhagic necrosis (11 of 11 mice within 3 d), followed by tissue healing (21–40 d) and cure (≤54 d; **Fig. 1a**). The cumulative cure rate was 64% (followed up to 90 d). Tumors in untreated ($n = 3$), light ($n = 4$) and dark ($n = 3$) controls continued to grow; mice were killed when the tumor reached ≥10% of body volume.

Photochemical generation of reactive oxygen species during the course of TOOKAD-PDT was confined mainly to the tumor blood vessels, as shown immunohistochemically by the anatomical distribution of the lipid peroxidation product 4-hydroxynonenal (HNE)[19], early after PDT (**Fig. 1b**). The strongest HNE staining was seen in large blood vessels located at the tumor rim (**Fig. 1b**). In light (**Fig. 1b**) and dark controls (data not shown), HNE staining was negative and seen only in the necrotic tumor core (spontaneous; PDT-independent).

It has been reported by us[3] and by others[4] that during the course of antivascular PDT, rapid and intense hemodynamic alterations and stasis are observed at the treated tumor site. We therefore assessed changes in tumor perfusion before, during and after PDT, using fluorescence intravital microscopy. TOOKAD administration and immediate tumor illumination initiated a rapid decrease in perfusion rate, reaching stasis in 3–4 min, whereas illumination alone had no significant effect (**Fig. 1c**).

Hemoglobin saturation in photosensitized blood

It was expected that photosensitization of circulating TOOKAD would lead to production of reactive oxygen species with concomitant oxygen depletion. We therefore examined acute changes in blood oxygenation, as manifested by changes in hemoglobin saturation levels (sPO_2), using two independent methods.

For the spectroscopic study, fresh human blood was subjected to spectral analysis of sPO_2 during PDT *in vitro*. Initial sPO_2 (in the dark) was ~65% (≤3 min; **Fig. 2a**). A rapid decline in sPO_2 was observed upon illumination, reaching a plateau at ~25% (≥2 min of illumination). In the absence of TOOKAD, illumination had no

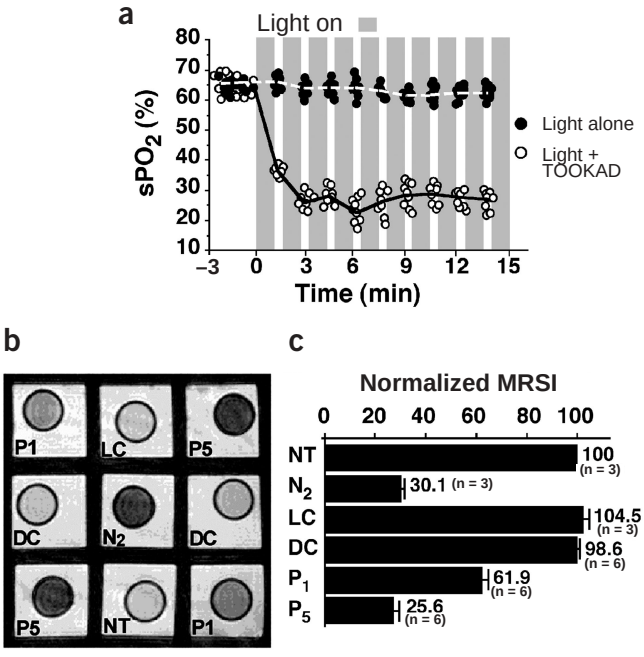

Figure 2 Photochemical reduction in sPO_2, recorded in human blood using TOOKAD and light. (**a**) Spectroscopy, with or without TOOKAD. To allow spectroscopic sPO_2 measurements, light was fractionated 10× (1 min light, 40 s dark) to enable eight repetitive 5-s readings each. (**b**) T_2-weighted MRI. Blood was photosensitized for 1 min (P_1, duplicate) or 5 min (P_5, duplicate); duplicates were positioned separately to minimize the influence of field inhomogeneity. NT, untreated blood; LC, light control (5 min); DC, dark control (duplicate); N_2, blood deoxygenated by N_2 equilibration. (**c**), MRSI changes with blood oxygenation (mean MRSI ± s.e.m). Experiments in **a**–**c** were repeated three times. **a** and **b** show representative experiments; **c** shows MRSI average ± s.e.m.

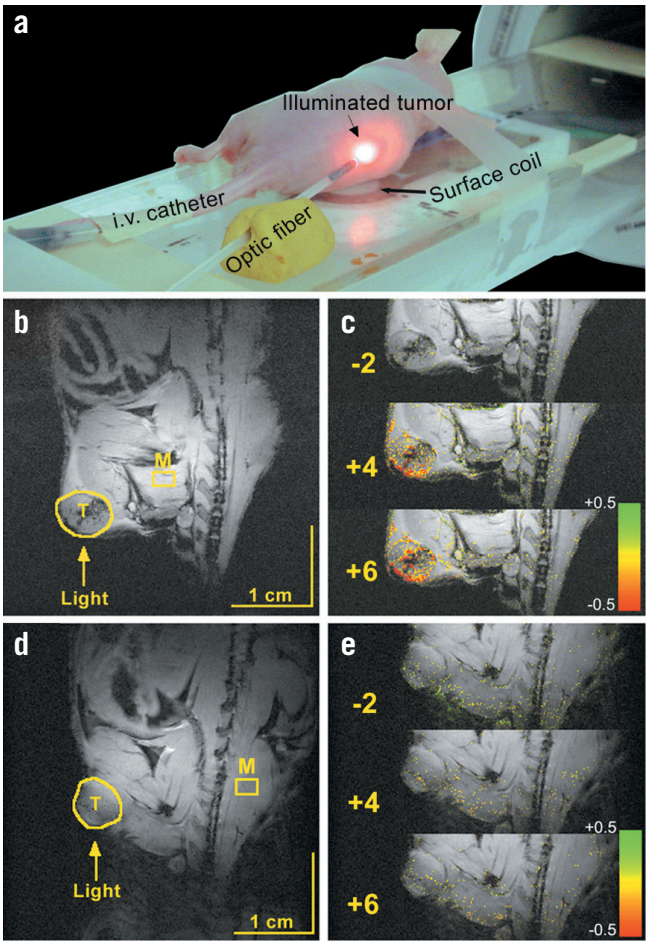

Figure 3 TOOKAD-PDT of M2R melanoma: online BOLD-contrast MRI. (**a**) Experimental setup used for remote intravenous TOOKAD administration and illumination inside the magnet. (**b**,**d**) Anatomical images (pre-PDT, gradient echo) of PDT-treated (**b**) and light-control (**d**) mice, showing tumor location (T), unilluminated muscle (M) and direction of sensitizing light beam (yellow arrows). (**c**,**e**) BOLD-contrast MR signal intensity maps of PDT-treated (**c**) and light-control (**e**) mice, superimposed on the corresponding anatomical images (**b** and **d**, respectively) at the indicated time points (–2, +4 and +6 min), relative to onset of illumination. Color-coded maps represent the logarithmic ratio of signal intensity over baseline. The reduction in signal intensity upon illumination of the TOOKAD-treated mouse (**c**; +4 and +6 min) is solely confined to the illuminated zone, whereas no contrast is generated in the absence of TOOKAD (**e**) or light (M). Representative experiments are shown ($n = 6$ for PDT and $n = 4$ for light control).

effect. These results indicate that photosensitization with TOOKAD in blood leads to a reduction in sPO_2.

We next determined the effect of PDT on sPO_2 in isolated human blood, as manifested in T_2-weighted magnetic resonance signal intensity (MRSI) under similar conditions. MRSI declined by 38.1% and 74.4% after 1 and 5 min of illumination, respectively, reaching a basal level equivalent to that of deoxygenated blood equilibrated with N_2 (**Fig. 2b**,**c**). MRSI of dark and light controls was essentially identical to that of untreated blood, which was defined as 100%. Thus, photosensitization of TOOKAD in blood reduces sPO_2, as reflected by a significant decrease in MRSI of T_2-weighted magnetic resonance images in the absence of flow and volume changes.

BOLD-contrast MRI during solid tumor PDT

Having shown that photosensitization of TOOKAD induces changes in blood oxygen levels, we next attempted to detect such changes during PDT of a solid tumor *in vivo*, using MRI. BOLD-contrast MRI was applied before, during and after PDT of a solid subcutaneous melanoma tumor (**Fig. 3**; see **Fig. 3a** for experimental setup and **Fig. 4** for quantitative analysis). TOOKAD administration with illumination induced a profound decrease in MRSI (25–40%) solely within the illuminated tumor area (**Figs. 3c** and **4a**). The strongest decrease in MRSI was observed at the tumor rim (**Fig. 3c**), in agreement with the spatial pattern of PDT-induced lipid peroxidation (**Fig. 1b**). No detectable change in MRSI was observed in unilluminated muscle (**Figs. 3b**,**c** and **4a**) or in the light (**Figs. 3d**,**e** and **4b**) and dark tumor controls (**Fig. 4c**). Attenuation of MRSI developed during the first 6–7 min of illumination and remained low throughout the experiment. These results suggest that rapid (≤2 min), local, photosensitized magnetic resonance BOLD contrast is generated during PDT. It also seems that the decline in perfusion rate and the changes in MRSI follow a similar kinetic pattern (**Figs. 4a** and **1c**), suggesting that vascular shutdown is a major factor contributing to the light-dependent changes in magnetic resonance contrast.

Multiecho gradient echo (MEGE) is a method for distinguishing between changes in blood oxygenation and flow effects[18]. MEGE revealed a rapid increase in ΔR2* (defined as $R_2^*{}_{illumination} - R_2^*{}_{preillumination}$)upon photosensitizer administration and illumination (**Fig. 4d**). This result implies that the decrease in MRSI (**Fig. 4e**) may be attributed, at least in part, to a reduction in blood oxygenation. The different recovery dynamics for R2* and MRSI may

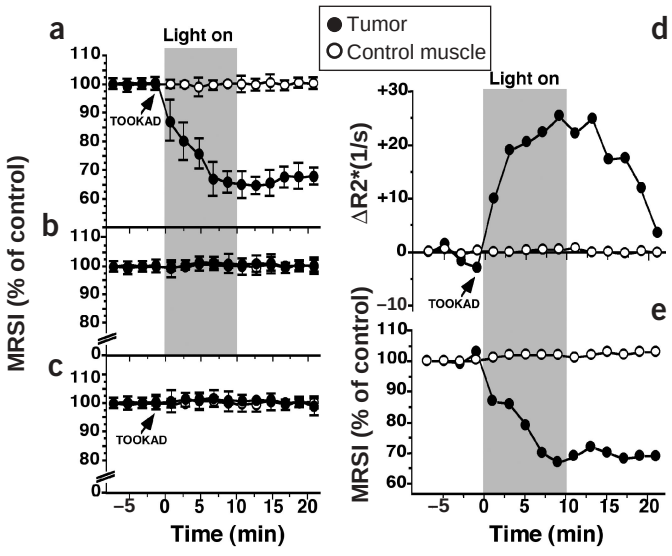

Figure 4 Kinetics of changes in BOLD-contrast MRI during TOOKAD-PDT. (**a**–**c**) Normalized MRSI (% of baseline at t_0 ± s.e.m.) was calculated from tumors and unilluminated control muscle (**Fig. 3**, T and M, respectively), in PDT-treated (**a**; $n = 6$), light-control (**b**; $n = 4$) and dark-control (**c**; $n = 4$) mice. (**d**) ΔR2* reflects changes in blood oxygenation and is independent of flow effects. R2* maps were derived by weighted linear regression of ln(MRSI) from data acquired using MEGE. (**e**) The rapid increase in ΔR2* upon drug administration and illumination (**d**) correlates with reduction in MRSI in the tumor ($n = 4$). No significant changes in MRSI or ΔR2* were observed in the light-control mice ($n = 4$). **d** and **e** show representative data from the same mouse.

reflect changes in the coupling between reduced blood flow (culminating in stasis), volume (evolving vasoconstriction, >2–3 min after onset of illumination) and photochemical and metabolic oxygenation after the termination of illumination.

DISCUSSION

The results of our study show that intravascular photosensitization of TOOKAD generates a change in BOLD contrast that is detectable by MRI. TOOKAD-PDT of mouse melanomas led to a 25–40% decline in MRSI (**Fig. 4a**,**e**), solely confined to the illuminated tumor zone (**Fig. 3c**). We suggest that this phenomenon results mainly from two processes that act in concert. First, rapid photochemical oxygen consumption leads to a rapid decline in sPO_2 (~75% within the first minute of illumination; **Fig. 2a**), as shown by spectral analysis and by the reduction MRSI in T_2-weighted MRI of blood without changes in flow or volume (74.4% at 5 min of illumination; **Fig. 2b**,**c**). This deoxygenation of hemoglobin was also expected to significantly contribute to changes in bulk magnetic susceptibility, consistent with the changes in T_2^*-weighted BOLD contrast observed *in vivo* (**Figs. 3c** and **4d**,**e**). These results were consistent with our previous report in which tissue oxygenation during PDT was directly measured in the same tumor model using an optical oxygen sensor[1]. Second, a rapid hemodynamic effect, manifested by local vascular occlusion and stasis, was revealed by intravital microscopy (**Fig. 1c**). This process prevents local reoxygenation, thereby resulting in enhancement of the photochemically generated magnetic resonance contrast[14]. Reduced blood flow may further attenuate MRSI by reducing inflow effects (T_1 contrast). Consequently, our results suggest that the observed changes in BOLD contrast are the result of contributions by both photochemical and hemodynamic effects exclusively reporting from within the bloodstream, where photosensitization takes place. The kinetics of the two processes are similar (**Figs. 1c** and **2a**,**c**) but their relative contribution to the overall decline in MRSI (**Fig. 4a**) has yet to be established. It seems that these two processes are closely related in time and space, as judged by independent criteria (BOLD-contrast MRI, lipid peroxidation immunohistochemistry and intravital microscopy).

These results describe, for the first time, functional imaging of solid tumor treatment using BOLD-sensitive parameters that could be applied to the online monitoring of clinical PDT. New intraoperative applications might be suggested for PDT of internal tumors (such as prostate, lung and brain). Photosensitized BOLD-contrast MRI could provide accurate three-dimensional monitoring of tumor vascular insult, the hallmark of antivascular PDT. In addition, careful calibration of the early photochemically induced changes in BOLD contrast (at various photosensitizer and light doses) could yield a correlative index for predicting the extent of photodynamic damage. This could permit interactive adjustment of treatment intensity for optimizing treatment outcome.

In the case of internal tumors, where light is interstitially delivered, avoiding damage to neighboring organs or major blood vessels requires precise delivery of light. Thus, the concept of photosensitized functional MRI could be applied to guided-light delivery, which would permit interactive adjustment to the direction and intensity of the light beam. Because of the appreciable depth of TOOKAD photosensitization *in vivo*[10,11], functional guidance might be effective for a few centimeters around the interstitial optic fiber. Consequently, future development of this imaging technology should be aimed at obtaining detectable changes in BOLD contrast in the presence of subdestructive delivery of attenuated photosensitizer and light doses. This seems feasible, as photochemical oxygen depletion is almost instantaneous[1] (**Fig. 2a**) and photosensitized magnetic resonance BOLD contrast is of an extremely high magnitude (**Figs. 3c** and **4a**), being about tenfold higher than reported for physiological activation of brain function (~5%)[20] and comparable to vasoactively induced stimuli affecting BOLD contrast in tumors[16,17].

In BOLD-contrast neuroimaging, outflow of deoxygenated blood from the activated area gives rise to 'false-positive' BOLD signals extending beyond the activated region (downstream dilution effect)[21]. Indeed, in the case of PDT, the current MRI protocol might also suffer from this effect. To minimize this undesired effect, we suggest that future development of this technology should be aimed at delivery of pulsed light, gated with rapid MRI sequences. In a typical setup, each illumination pulse would be terminated at the end of acquisition of each phase-encoding step, so light would be delivered only during time to echo (TE), consisting of only a fraction of the repetition time. Such a setup could ensure that light would be mostly 'off' during MRI data acquisition, minimizing vascular damage and the potential contribution of downstream spread of deoxygenated blood to the magnetic resonance readout.

In light of the fact that intraoperative open-magnet MRI is being widely used for controlling complex surgical procedures (reviewed in ref. 22), our results suggest that with some further development and careful calibration, photosensitized MRI could provide the means for real-time guidance and assessment of PDT.

METHODS

Animals, tumor model and PDT. Protocols of animal experiments were reviewed and approved by the Institutional Animal Care and Use Committee of the Weizmann Institute of Science. Male CD1-nude mice (30 ± 2 g) were implanted subcutaneously with M2R melanoma xenografts[3]. PDT was done on 7- to 9-mm tumors as previously described[3,8], with the following changes: intravenous administration of TOOKAD (5 mg/kg in vehicle; Steba Biotech) was immediately followed by fiber-optic guided tumor illumination (light spot ϕ = 1 cm^2, 763 nm, 102 J/cm^2 for 10 min, using a 1-W diode laser; CeramOptec). Under these conditions, skin or tumor temperatures (by thermocouple) did not increase by more than 1 °C.

PDT was done in three modes. For tumor therapy, intravenous TOOKAD administration was immediately followed by transcutaneous illumination. For MRI, TOOKAD administration (by remotely activated intravenous catheterization) and transcutaneous illumination were done inside the magnet (**Fig. 3a**). For intravital microscopy, TOOKAD administration and illumination of the pre-exposed subcutaneous tumor from the inner face of the skin (skin-flap model[23]) were conducted on the microscope stage. We used light controls (illuminated tumors in mice treated with vehicle alone) and dark controls (TOOKAD administered without illumination). Mice were killed with CO_2 when tumors reached ≥10% of body volume.

MRI experiments. Gradient echo and MEGE magnetic resonance images were acquired on a horizontal 4.7-T Bruker BioSpec spectrometer as previously described[17] (TE 10 ms for gradient echo and TE 10, 21.24 and 32.48 ms for MEGE, repetition time 230 ms, flip angle 40°, 256 × 256 pixels).

For animal studies, a whole-body excitation coil and a radiofrequency-decoupled 1.5-cm surface coil were used to improve signal-to-noise ratio (field of view 4 cm, slice thickness 0.8 mm). Mice were anesthetized, catheterized and restrained by adhesive tape (supine/lateral) to position the tumor above the center of the MRI surface coil; the laser optic fiber was fixed in place to illuminate the tumor area (**Fig. 3a**). After acquisition of four sequential images, mice were intravenously injected with TOOKAD, followed by illumination (10 min) while 11 more images were acquired. Room temperature was maintained at 28 °C.

For *ex vivo* measurements, freshly collected human blood in sodium citrate was spun down and resuspended in autologous plasma to 0.6–0.7 hematocrit, to minimize red blood cell sedimentation during MRI experiments. Blood

samples (500 µl) were placed in 6 × 50 mm glass tubes (Kimble) sealed under N_2, and each was placed in a 3.5-ml optical plastic cuvette containing 2 ml of PBS. A proton-volume coil was used (field of view 7 cm, slice thickness 2 mm, data zero filled to 512 × 512). Data were analyzed as the mean MRSI of the blood sample relative to the surrounding PBS.

Data analysis. MRI data was analyzed using MATLAB (MathWorks), Orisis (version 4.0.9; University Hospital of Geneva) and Paravision 2.1.1 (Bruker). R2* maps were derived by noise-weighted linear regression of log(MRSI) for each pixel. Only pixels with a fit of $R^2 \geq 0.36$ were analyzed.

Immunohistochemistry. Immunohistochemistry of PDT-induced lipid peroxidation was based on immunodetection of HNE, an aldehydic peroxidation product of polyunsaturated fatty acids that forms covalent adducts with proteins by reductive amination and Michael-type addition[19]. Immunohistochemistry was done using rabbit antiserum to HNE (1:400; Calbiochem)[19], horseradish peroxidase–conjugated goat secondary antibody to rabbit IgG (Jackson) and 3-amino-9-ethylcarbazole (Sigma) as a chromogenic substrate.

Measurement of sPO_2 of photosensitized blood using optical spectroscopy. Fresh human blood collected in sodium citrate was steered at 37 °C in a sealed optical cuvette under N_2, without or with TOOKAD (100 µg/ml). Online spectroscopic sPO_2 determination was done with a LESA reflectance spectrometer (BioSpec)[24]. Recording was initiated 2 min before illumination. Ten illumination cycles (1 min each, 170 mW/cm^2) were carried out, with spectral measurements (8 × 5 s) in the intervening periods when the light was turned off.

Intravital microscopy. Fluorescence intravital microscopy was done with an upright microscope (Nikon Optiphot-2) equipped with a thermoregulated stage (37 °C), a CCD camera (50 frames per second; Applitech) and a VCR (JVC model HR-J437MS) for video recording. Red blood cell flux was monitored in M2R tumors exposed on the inner skin face (wetted with saline) using the skin-flap model[23]. Red blood cells from a donor mouse were labeled *ex vivo* with 4-(4-(didecylamino)styryl)-*N*-methylpyridinium iodide (4-Di-10-ASP; 7.5 µg/ml; Molecular Probes)[24,25]. Labeled red blood cells mixed with TRITC-dextran (256 kDa, 0.5 mg/mouse as blood-pool marker; Sigma) were intravenously administered to the tumor-bearing mice (labeled cells comprised 1.17 ± 0.08% of host red blood cells, as verified on blood smears) and allowed to circulate for 10 min before video recording. Recording (magnification ×100, 20 min) started 5 min before TOOKAD administration and illumination and ended 5 min after the light was turned off. Mice were killed using CO_2 at the end of the experiment.

ACKNOWLEDGMENTS

Y.S. is the incumbent of the Tillie and Charles Lubin Professorial Chair in Biochemical Endocrinology. A.S. is the incumbent of the Robert and Yadele Sklare Professional Chair in Biochemistry. S.G and A.G. are in partial fulfilment of their Ph.D. theses at the Feinberg Graduate School of the Weizmann Institute of Science. We wish to acknowledge the technical help of I. Meerovitch and Y. Machluf. This work was supported by Steba Biotech.

COMPETING INTERESTS STATEMENT

The authors declare competing financial interests (see the *Nature Medicine* website for details).

Received 26 September 2002; accepted 2 August 2003
Published online at http://www.nature.com/naturemedicine/

1. Zilberstein, J. *et al.* Light-dependent oxygen consumption in bacteriochlorophyll-serine-treated melanoma tumors: on-line determination using a tissue-inserted oxygen microsensor. *Photochem. Photobiol.* **65**, 1012–1019 (1997).
2. Sitnik, T.M., Hampton, J.A. & Henderson, B.W. Reduction of tumor oxygenation during and after photodynamic therapy *in vivo*: effects of fluence rate. *Br. J. Cancer* **77**, 1386–1394 (1998).
3. Zilberstein, J. *et al.* Antivascular treatment of solid melanoma tumors with bacteriochlorophyll-serine-based photodynamic therapy. *Photochem. Photobiol.* **73**, 257–266 (2001).
4. Dolmans, D.E. *et al.* Vascular accumulation of a novel photosensitizer, MV6401, causes selective thrombosis in tumor vessels after photodynamic therapy. *Cancer Res.* **62**, 2151–2156 (2002).
5. Hopper, C. Photodynamic therapy: a clinical reality in the treatment of cancer. *Lancet Oncol.* **1**, 212–219 (2000).
6. Dougherty, T.J. An update on photodynamic therapy applications. *J. Clin. Laser Med. Surg.* **20**, 3–7 (2002).
7. Scherz, A., Salomon, Y., Scheer, H. & Brandis, A. Palladium-substituted bacteriochlorophyll derivatives and use thereof. US Patent 6,569,846 (2003).
8. Schreiber, S., Gross, S., Harmelin, A., Scherz, A. & Salomon, Y. Local photodynamic therapy (PDT) of rat C6 glioma xenografts with Pd-bacteriopheophorbide leads to decreased metastases and increase of animal cure compared to surgery. *Int. J. Cancer* **99**, 279–285 (2002).
9. Kelleher, D.K. *et al.* Water-filtered infrared-A radiation: a novel technique for localized hyperthermia in combination with bacteriochlorophyll-based photodynamic therapy. *Int. J. Hyperthermia* **15**, 467–474 (1999).
10. Chen, Q. *et al.* Preclinical studies in normal canine prostate of a novel palladium-bacteriopheophorbide (WST09) photosensitizer for photodynamic therapy of prostate cancer. *Photochem. Photobiol.* **76**, 88–95 (2002).
11. Koudinova, N. *et al.* Photodynamic therapy with Pd-bacteriopheophorbide (TOOKAD): successful *in vivo* treatment of human prostatic small cell carcinoma xenografts. *Int. J. Cancer* **104**, 782–789 (2003).
12. Preise, D. *et al.* Bypass of tumor drug resistance by antivascular therapy. *Neoplasia* (in the press).
13. Ogawa, S. & Lee, T.M. Magnetic resonance imaging of blood vessels at high fields: *in vivo* and *in vitro* measurements and image simulation. *Magn. Reson. Med.* **16**, 9–18 (1990).
14. Turner, R. Signal sources in BOLD contrast fMRI. *Adv. Exp. Med. Biol.* **413**, 19–25 (1997).
15. Taylor, N.J. *et al.* BOLD MRI of human tumor oxygenation during carbogen breathing. *J. Magn. Reson. Imaging* **14**, 156–163 (2001).
16. Abramovitch, R., Marikovsky, M., Meir, G. & Neeman, M. Stimulation of tumour angiogenesis by proximal wounds: spatial and temporal analysis by MRI. *Br. J. Cancer* **3**, 440–447 (1998).
17. Gilead, A. & Neeman, M. Dynamic remodeling of the vascular bed precedes tumor growth: MLS ovarian carcinoma spheroids implanted in nude mice. *Neoplasia* **1**, 226–230 (1999).
18. Howe, F.A. *et al.* Issues in flow and oxygenation dependent contrast (FLOOD) imaging of tumours. Effects of different levels of hypercapnic hyperoxia on tumour R(2)* and arterial blood gases. *NMR Biomed.* **14**, 497–506 (2001).
19. Uchida, K. *et al.* Characterization of epitopes recognized by 4-hydroxy-2-nonenal specific antibodies. *Arch. Biochem. Biophys.* **324**, 241–248 (1995).
20. Detre, J.A. & Floyd, T.F. Functional MRI and its applications to the clinical neurosciences. *Neuroscientist* **7**, 64–79 (2001).
21. Turner, R. How much cortex can a vein drain? Downstream dilution of activation-related cerebral blood oxygenation changes. *Neuroimage* **16**, 1062–1067 (2002).
22. Jolesz, F.A. Interventional and intraoperative MRI: a general overview of the field. *J. Magn. Reson. Imaging* **8**, 3–7 (1998).
23. Yang, M. *et al.* direct external imaging of nascent cancer, tumor progression, angiogenesis, and metastasis on internal organs in the fluorescent orthotopic model. *Proc. Natl. Acad. Sci. USA* **99**, 3824–3829 (2002).
24. Neeman, M., Dafni, H., Bukhari, O., Braun, R.D. & Dewhirst, M.W. *In vivo* BOLD contrast MRI mapping of subcutaneous vascular function and maturation: validation by intravital microscopy. *Magn. Reson. Med.* **45**, 887–898 (2001).
25. Braun, R.D., Dewhirst, M.W. & Hatchell, D.L. Quantification of erythrocyte flow in the choroid of the albino rat. *Am. J. Physiol.* **272**, H1444–H1453 (1997).